Geomechanics and Engineering, *Vol. 21, No. 2 (2020) 143-152*
DOI: https://doi.org/10.12989/gae.2020.21.2.143

Earthquake risk assessment of underground railway station by fragility analysis based on numerical simulation

Sun Yong Kwon[§1a], Mintaek Yoo[§2b] and Seongwon Hong[*3]

[1]Division of Resources and Energy Assessment, Korea Environment Institute, 370 Sicheong-daero, Sejong-si, Republic of Korea
[2]Railroad Structure Research Team, Korea Railroad Research Institute, Euiwang, 360-1 in Wolam-dong, Uiwang-si, Gyeonggi-do, Republic of Korea
[3]Department of Safety Engineering, Korea National University of Transportation, 50 Daehak-ro, Chungju-si, ChungBuk 27469, Republic of Korea

(Received December 11, 2019, Revised February 10, 2020, Accepted March 2, 2020)

Abstract. Korean society experienced successive earthquakes exceeding 5.0 magnitude in the past three years resulting in an increasing concern about earthquake stability of urban infrastructures. This study focuses on the significant aspects of earthquake risk assessment for the cut-and-cover underground railway station based on two-dimensional dynamic numerical analysis. Presented are features from a case study performed for the railway station in Seoul, South Korea. The PLAXIS2D was employed for numerical simulation and input of the earthquake ground motion was chosen from Pohang earthquake records (M5.4). The paper shows key aspects of earthquake risk for soil-structure system varying important parameters including embedded depth, supported ground information, and applied seismicity level, and then draws several meaningful conclusions from the analysis results such as seismic risk assessment.

Keywords: earthquake risk assessment; underground structure; railway station; damage index; numerical analysis

1. Introduction

Underground structure is important infrastructure especially in urban area and widely utilized as tunnels, pipes, metro stations, parking lots, and complex shopping malls. In South Korea, new facilities have been constructed in underground spaces to overcome shortage of land space and significance of appropriate design approach for underground structure is very strengthened. On the other hands, Korean society experienced successive earthquakes exceeding 5.0 magnitude in couple of years and Gyeong-ju earthquake (M5.7 2016) was the largest earthquake ever recorded in South Korea. It caused significant concerns in stability of major facilities in urban area induced by earthquake, and seismic design criteria for many facilities have been extensively revised.

Underground structure is known as a relatively safe system under earthquake (Okamoto 1973). However, it was reported that underground structure also can be significantly damaged or collapsed during earthquake (Hashash *et al.* 2001, Pitilakis and Tsinidis, 2014, Roy and Sarkar, 2017) and several studies as Sevim (2013), Fattah *et al.* (2015), Liu *et al.* (2015), Ozturk *et al.* (2016), Liu *et al.* (2018) were performed to investigate dynamic behavior of tunnel during earthquake. Damage on underground structure was examined both in qualitative and quantitative ways. Qualitative method was described in ALA (2001), Dowding and Rozan (1978), FEMA (2003), and Werner *et al.* (2006). In these studies, damage state was categorized by series of built-in modules containing various information as structure inventory, structure vulnerability, seismic requirements with high/moderate/low code seismic, and so on. In the stage of scoring each term, treat of uncertainty was approximate inevitably. In quantitative manner, fragility of excavated tunnel in rock was estimated by width and length of crack (Corigliano *et al.* 2007) and rotational angle of the structure (Andretti *et al.* 2013, Andreotti and Carlo 2014). Lee *et al.* (2016) and Park *et al.* (2018) defined damage index as the ratio of predicted moment to the yield moment. Based on damage index, damage state can be defined as minor, moderate, and extensive states, which represent the damage condition of structures according to the level of induced earthquake level such as return period. It is useful tool which can be applied to estimate the seismic performance of infrastructures and many buildings, but utilization in the underground railway station, which is major underground structure in many metropolitan cities, is very limited. Damage index can be divided into two methods: empirical and numerical methods. ALA (2001) and FEMA (2003) provided the representative empirical damage state based on empirical method. However, these damage index had a limitation because they were drawn based on the limited available data and it was impossible to determine the system having various soil conditions and tunnel types. To overcome this issue, the development of damage index

*Corresponding author, Professor
E-mail: shong@ut.ac.kr
[a]Research Fellow
[b]Senior Researcher

[§]Both authors contributed equally to this manuscript

ISSN: 2005-307X (Print), 2092-6219 (Online)

using numerically obtained data was required.

In this study, damage index for underground railway station structure were derived in various site conditions. Primary parameters including embedded depth of railway station, supported ground information, and applied seismicity level were varied and employed for analysis with 33 cases. In addition, damage state of underground structure according to hazard intensity was also suggested. Each case was set to reflect the revised Korean seismic design criteria (Ministry of Interior and Safety 2017). Numerical simulation was carried out for all 33 cases to obtain input data of damage index based on two-dimensional finite element method. The PLAXIS2D was chosen as a simulation tool, and base input earthquake motion was artificially set from Pohang earthquake records (M5.4). The paper highlights key aspects of seismic behavior of soil-structure system and draws several meaningful conclusions from the analysis results.

2. Numerical modeling method and condition

In this study, seismic responses of underground railway station were calculated by PLAXIS2D, which is two-dimensional numerical simulation tool. Model system was simulated virtually based on the OOO Station, which is underground railway station located in Seoul, South Korea. Schematic view of the target system is depicted in Fig. 1. Railway station was composed of 2 floors with the width of 22m and the height of 10 m, and was fabricated by reinforced concrete. Structural section and material properties of the railway station are presented in Fig. 2 and Table 1, respectively. Primary parameters which were expected to have a relatively significant impact on the seismic behavior was selected for case formulation of numerical study, which were soil condition, depth of the base rock, depth of the railway station, and seismic intensity. Finally, 33 analysis cases were constituted and summarized in Table 2 and Fig. 3. In Table 2, soil classes were categorized from S1 to S5 to describe the revised Korean seismic design criteria (Ministry of Interior and Safety, 2017). The S1, S2, S3, S4, and S5 denotes rock based ground, shallow and stiff ground, shallow and soft ground, deep and stiff ground, and deep and soft ground, respectively, as shown in Table 3.

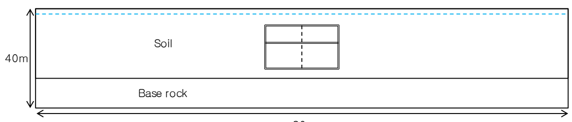

Fig. 1 Schematic view of target system

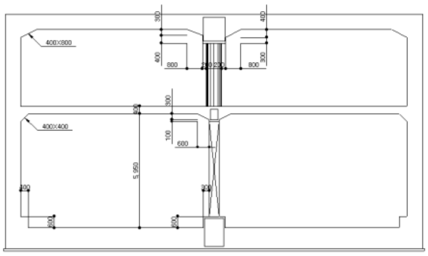

Fig. 2 Structural section of target railway station

Table 1 Material properties of railway station

Concrete stiffness(MPa)	24	Elastic modulus of steel(MPa)	200,000
Elastic modulus of concrete(MPa)	26,950	Unit weight of reinforced concrete(kN/m^3)	25
Steel stiffness(MPa)	300	Spacing of center column(m)	5

Table 2 List of the analysis cases

Case number	Soil class	Depth of the base rock (m)	Depth of the railway station (m)	Vs of soil (m/s)	Return period of Input earthquake motion(year)
1	S1	0.8	1	360	500
2	S2	16	1	360	
3			6		
4	S3	16	1	150	
5			6		
6	S4	30	11	360	
7			15		
8			21		
9	S5	30	11	150	
10			15		
11			21		
12	S1	0.8	1	-	1000
13	S2	16	1	360	
14			6		
15	S3	16	1	150	
16			6		
17	S4	30	11	360	
18			15		
19			21		
20	S5	30	11	150	
21			15		
22			21		
23	S1	0.8	1	-	2400
24	S2	16	1	360	
25			6		
26	S3	16	1	150	
27			6		
28	S4	30	11	360	
29			15		
30			21		
31	S5	30	11	150	
32			15		
33			21		

Hardening soil model with small strain stiffness (HSSMALL) was adopted for soil constitutive model (Plaxis, 2016). This criterion can consider stress dependency of soil shear modulus and hysteretic damping which can simulate nonlinearity of shear modulus and

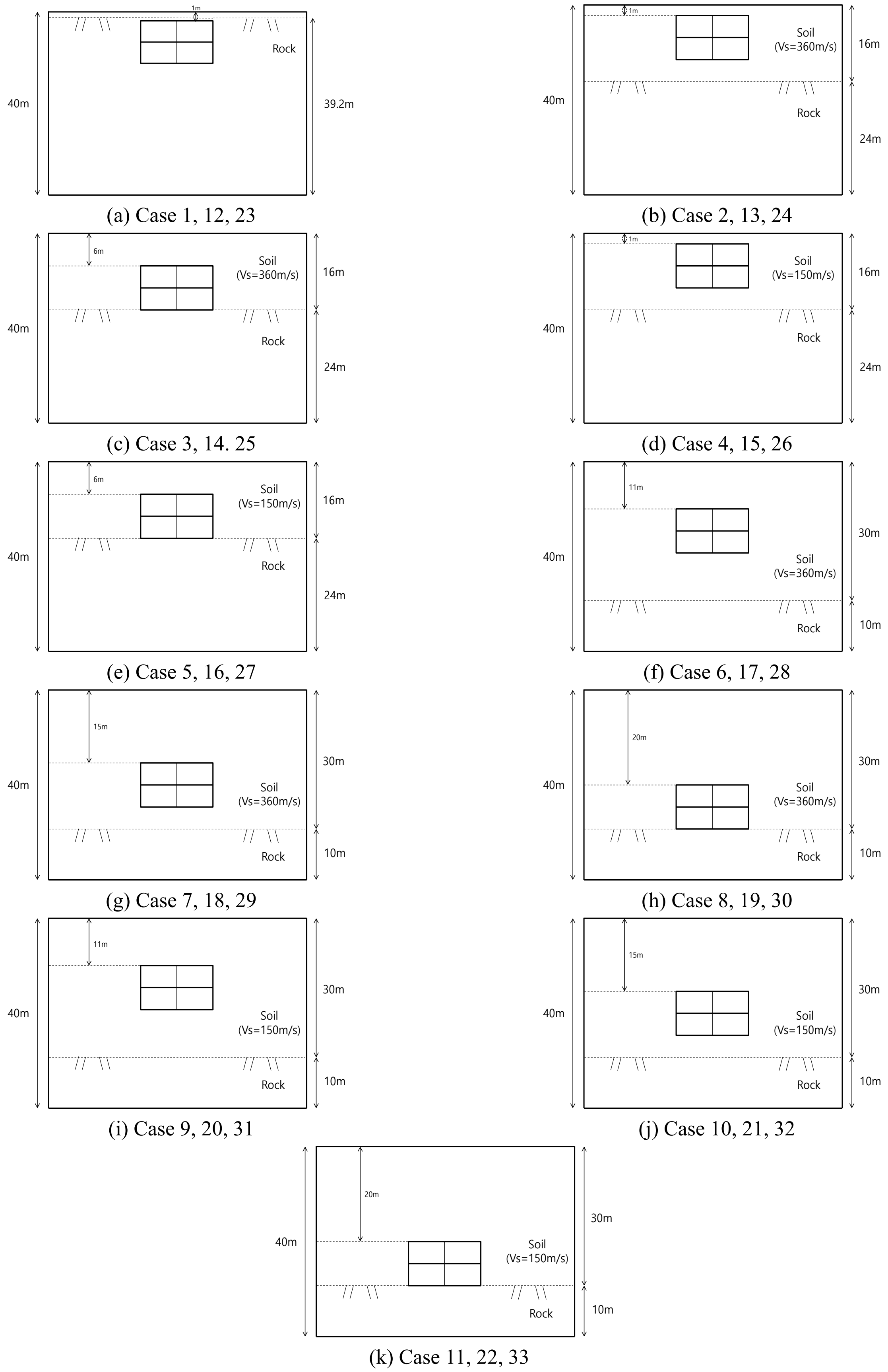

Fig. 3 Schematic view of the analysis cases

damping ratio as increase of shear strain was applied. Ground water level was located at 1m below ground surface and detailed geotechnical properties were summarized in Tables 4 and 5. In Table 4, primary input parameters used in

Table 3 Categorization of soil classes (Ministry of Interior and Safety 2017)

Soil class	Address of soil class	Criteria of categorization	
		Depth of base rock, H (m)	Average shear wave velocity of soil ($V_{s,soil}$, m/s)
S_1	Rock based ground	H < 1 m	-
S_2	Shallow and stiff ground	1m ≤ H ≤ 20 m	$V_{s,soil} \geq 260$ m/s
S_3	Shallow and soft ground		$V_{s,soil} < 260$ m/s
S_4	Deep and stiff ground	H > 20 m	$V_{s,soil} \geq 180$ m/s
S_5	Deep and soft ground		$V_{s,soil} < 180$ m/s

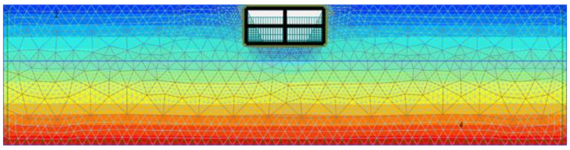

Fig. 4 Modeling mesh of target system (Case 2)

Table 4 Material properties of model soil (Ministry of Interior and Safety 2017)

Parameters	Soil (Vs=150 m/s)	Soil (Vs=360 m/s)
Void ratio	0.95	0.25
Poisson's ratio	0.2	0.3
Dry unit weight (kN/m^3)	13.8	22.0
Friction angle (˚)	24	40
Cohesion (kN/m^2)	10	10
dilatancy angle (^{o})	0	0
R_{inter}	0.67	0.67
ϒ at which G_s=0.722G_0	0.00015	0.0007

Table 5 Material properties of base rock (Ministry of Interior and Safety 2017)

Unit weight (kN/m^3)	23
Elastic modulus (kN/m^2)	3,600,000
Friction angle (˚)	42
Cohesion (kN/m^2)	300

HSSMALL model were artificially created and adjusted by matching with Korean seismic design criteria (Ministry of Interior and Safety 2017). Fig. 4 exhibits the example of representative modeling mesh of target system (Case 2) used to calculate seismic responses of underground railway station in this study. Walls and slabs of the underground railway station fabricated with reinforced concrete were modeled by 2D plate element, and center columns were modeled by node-to-node anchor element with spacing of 5 m. Primary properties used in each structural model as flexural rigidity and axial stiffness were estimated based on the material properties summarized in Table 1. Interface elements were adopted at the interface between plate and soil elements to simulate dynamic interaction effect such as stiffness degradation at soil-structure interface under earthquake (R_{inter}=2/3). Separation, overlapping, and slippage of the soil and structure were simulated in the interface model. Soil and base rock was modeled with identical solid element, and interface zone of the soil and rock media had no independent interface elements. Viscous boundary was applied for the lateral boundary condition of the model for proper simulation of energy dissipation. Dynamic analysis was then carried out based on two-dimensional plain strain condition and proceeded following steps according to the construction and loading phases: 1) static equilibrium of soil media, 2) construction of underground railway station and attainment of static equilibrium for overall system, and 3) dynamic analysis.

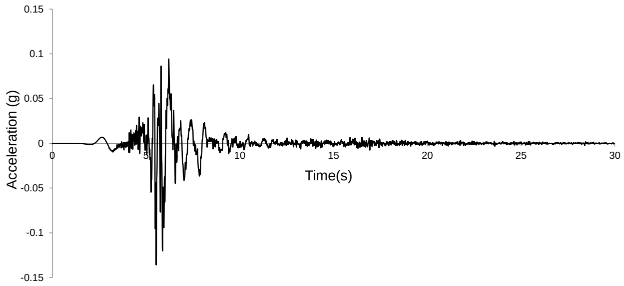

(a) Return period of 500 years

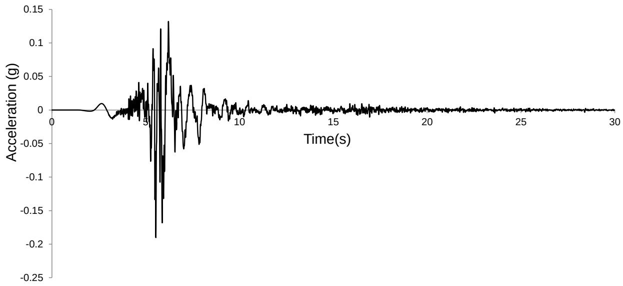

(b) Return period of 1000 years

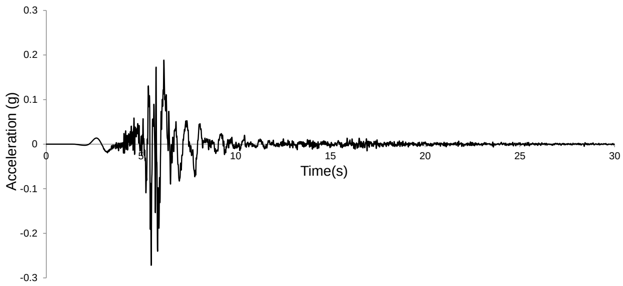

(c) Return period of 2400 years

Fig. 5 Time histories of input earthquake motion

Input earthquake motion used in this study was artificially created based on recorded values from Pohang earthquake (M 5.4, Observatory PHA2, NS direction), and spectrum amplitude was calibrated by Korean standard response spectrum (Ministry of Interior and Safety 2017). Three types of input earthquake motion were estimated according to the return period (500, 1000, 2400 years), and they were input at the bottom level of the model in the form of acceleration-time histories. Acceleration-time histories of each earthquake motion used in this study is shown in Fig. 5.

3. Results of numerical simulation

Repetitive analysis was carried out for every case shown

Table 6 Damage state

Damage state	Damage index, M/ M_d (Argyroudis and Pitilakis 2012)	Damage index M/M_y (Park *et al.* 2016)
None	DI < 1.0	DI < 1.0
Minor/slight	1.0 < DI < 1.5	1.0 < DI < 1.4
Moderate	1.5 < DI < 2.5	1.5 < DI < 2.3
Extensive	2.5 < DI <3.5	2.3 < DI

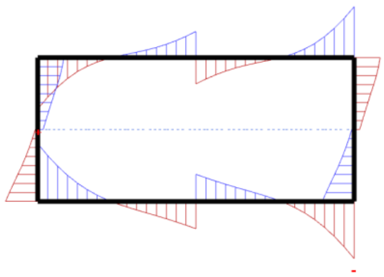

(a1) Maximum shear force profiles (V_{max} = 896.6 kN)

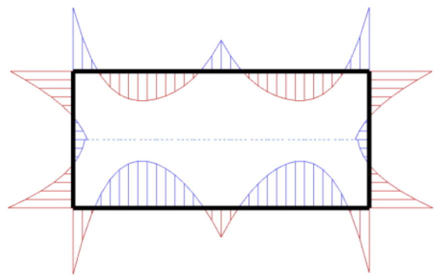

(a2) Maximum moment profiles (M_{max} = 1299 kN·m)

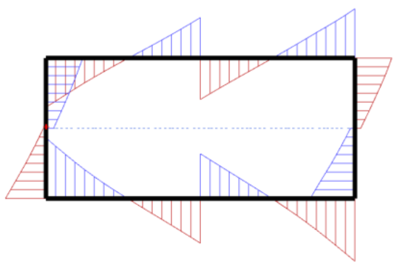

(b1) Maximum shear force profiles (V_{max} = 962.4 kN)

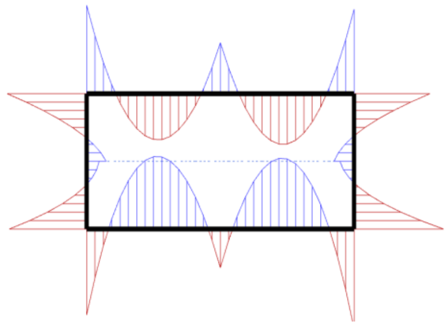

(b2) Maximum moment profiles (M_{max} = 1918 kN·m)

(b) Case 9

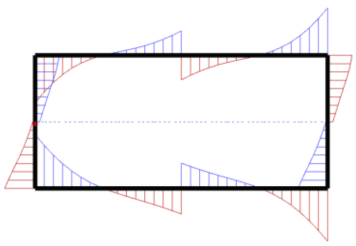

(c1) Maximum shear force profiles (V_{max} = 939.4 kN)

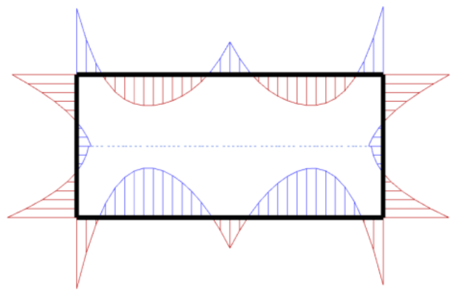

(c2) Maximum moment profiles (M_{max} = 1455 kN·m)

(c) Case 17

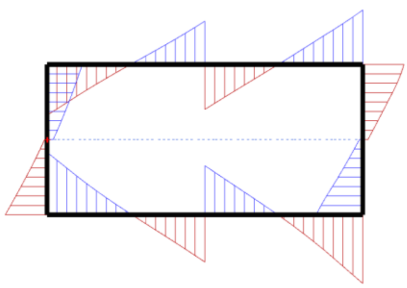

(d1) Maximum shear force profiles (V_{max} = 988.7 kN)

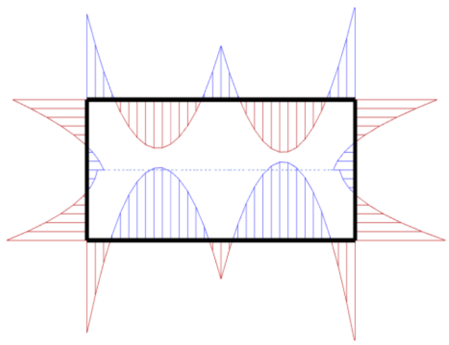

(d2) Maximum moment profiles (M_{max} = 2112 kN·m)

(d) Case 20

Fig. 6 Maximum shear force and bending moment profiles of underground railway station calculated from numerical simulation for Representative analysis cases in Table 2, and Fig. 6 demonstrates the representative maximum shear force, bending moment, and lateral displacement profiles of underground railway station for Cases 6, 9, 17, and 20. In these cases, station structure was located at identical depth but ground information and input earthquake level was different as Table 2 and Fig. 3. Trend of seismic response profiles was similar but detailed values at each critical location such as both ends of the slabs and walls was different because of the analysis condition.

Maximum seismic responses induced in Case 9 were generally larger than those in Case 6. It can be demonstrated that difference in soil stiffness caused difference in structural seismic responses. Shear wave velocity of Case 9 was much lower than that of Case 6, it can cause relatively larger site amplification effect in Case 9. These kinds of phenomenon also observed in Case 17, 20.

To investigate seismic ground responses which can significantly affect seismic behaviour of the underground structure, variation of input acceleration in the ground was analysed. Fig. 7 shows acceleration-time histories of the model ground according to the depth for Case 27 which has S3 soil and largest seismicity level (return period of 2,400 years). In the figure, acceleration responses were significantly varied for each observed location. Input earthquake motion with return period of 2400 years was properly induced at the bottom of the model as shown in Fig. 7(e). Then input motion was substantially amplified in rock media, and reached to peak response at the interface of soil and rock (Fig. 7(c), 7(d)). Amplified earthquake wave was slightly damped when it escape the soil-rock interface area, and somewhat re-amplified during approaching to the ground surface (Fig. 7(a), 7(b)). However site amplification effect in the soil media was somewhat limited. It is not typical phenomena because, in general, it is known that site amplification effect is dominant in soft soil layer not in rock layer. It seemed that this phenomenon occurred due to input earthquake characteristics and soil-rock interface effect. The Pohang earthquake was applied as input earthquake motion, and this earthquake motion was short period earthquake. In this kind of earthquake, response amplification can be occurred significantly in rock layer rather than in soft soil layer because of the frequency based wave characteristics. And earthquake wave can be significantly amplified when dynamic characteristic of medium is suddenly changed such as at the interface of soft soil and rock. This phenomenon can be seriously affect seismic responses of underground structure especially the target structure is located in rock media of at the soil-rock interface.

Overall, results from the 33 cases were derived, analysed by data tables and diagrams, and utilized for the damage index analysis for earthquake risk assessment of the underground railway station.

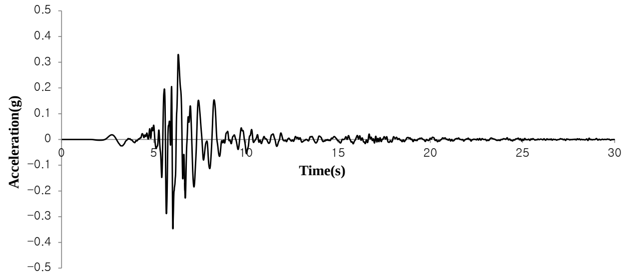

(a) Ground surface

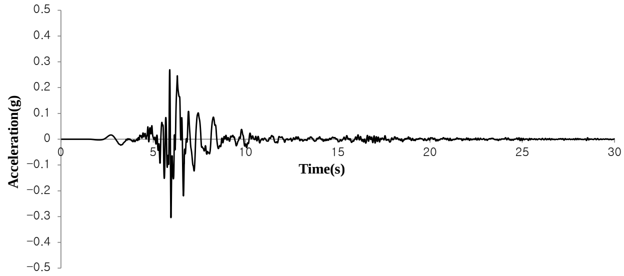

(b) Depth of 8.55 m (in soil media)

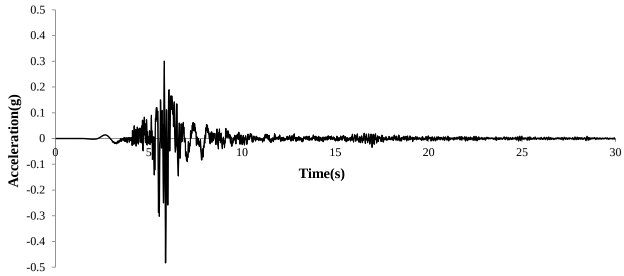

(c) Soil-rock interface

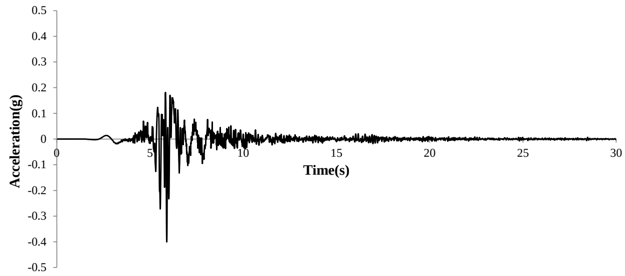

(d) Depth of 26 m (in rock media)

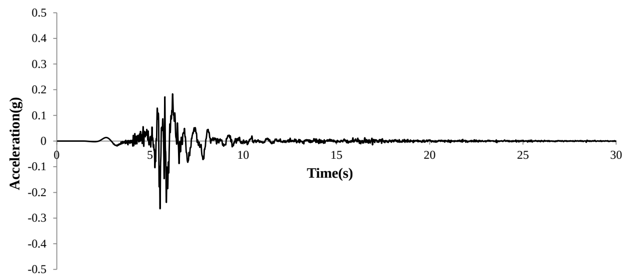

(e) Bottom of the model

Fig. 7 Ground acceleration-time history according to the depth (Case 27)

4. Damage index analysis of underground structure

Earthquake risk assessment was performed by comparing measured moment and shear force obtained from numerical analysis with yielding moment and allowable shear force of underground structure. Damage state of the underground structure could be classified three states as minor/slight, moderate, and extensive. Argyroudis and Pitilakis (2012) suggested damage index applying failure moment (M_d) and measuring moment at plastic hinge. In addition, damage state using ratio of measuring moment to

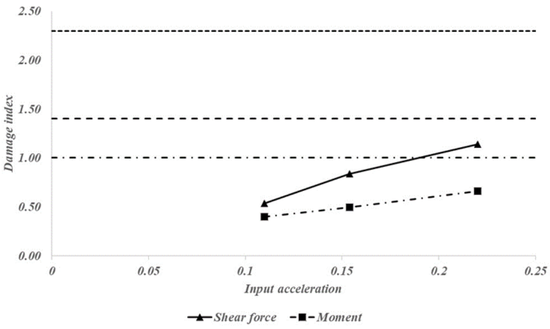

(a) Damage index for S1 soil

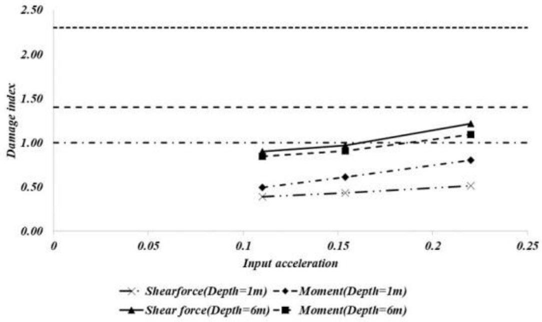

(b) Damage index for S2 soil

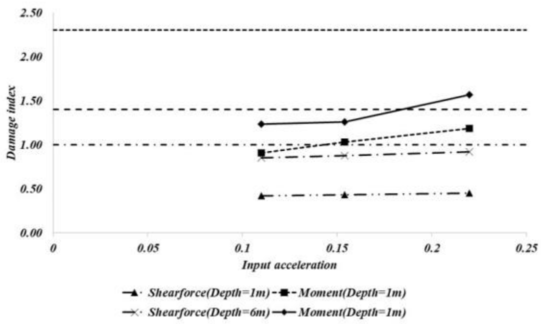

(c) Damage index for S3 soil

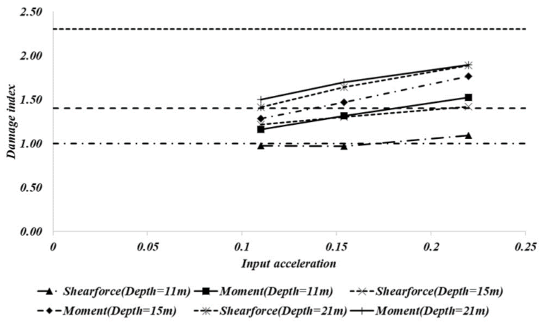

(d) Damage index for S4 soil

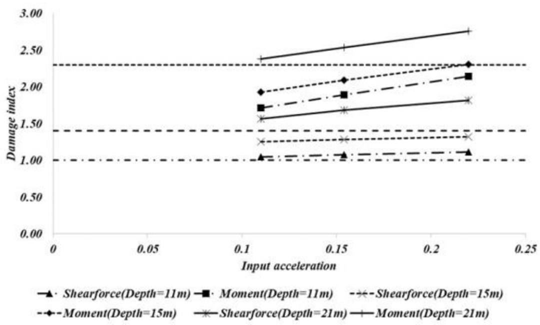

(e) Damage index for S5 soil

Fig. 8 Damage index analysis results

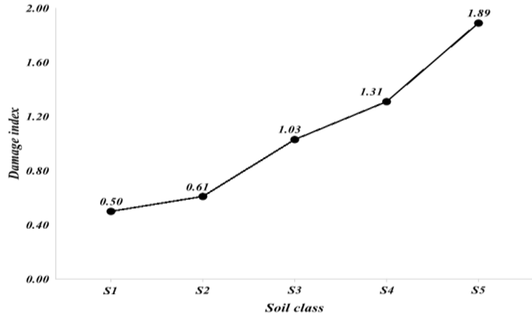

Fig. 9 Damage index for variation of soil class

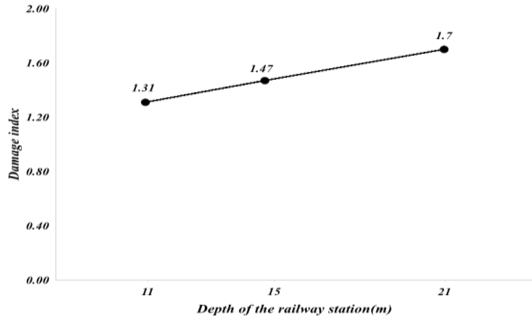

Fig. 10 Damage index for variation of depth of the railway station

yield moment (M_y) was developed by Park *et al.* (2016). When the damage state was determined using M_d value, predicted damage state was significantly conservative comparing actual seismic performance. Therefore, in this study, M_y was applied for determining damage state to consider performance uncertainty of reinforced concrete structure (Park *et al.* 2016). Damage state from shear force was determined using same criteria with yield moment. Yield moment and allowable shear force value was referred in design document of tunnel structure. The damage states of preceded research were summarized in Table 6.

Base on numerical analysis results, damage index values were calculated for each case using damage state of Park *et al.* (2016). Fig. 8 describes the damage index results for each soil classification. Underground railway station in S1 soil (Fig. 8(a)) could be damaged slightly when the earthquake with return period of 2,400 years occurred. In Case of S2 soil deposit (Fig. 8(b)), case with 6m depth of railway station could be damaged slightly as the earthquake with return period of 2,400 years occurred. The damage index value in case with depth of 6m is higher than that in case with depth of 1m. It denotes that the observed moment and shear force of deep structure were higher than that of shallow structure. In addition, the lower member of underground structure was placed at soil-rock layer interface in case with depth of 6m, and the structural moment from earthquake tends to increase at that location.

This phenomenon reflects input earthquake characteristics and soil-rock interface effect presented in Fig. 7. In case of S3 soil (Fig. 8(c)), similar trends were also observed in S2 soil case. In addition, the moment damage index exceeded 1.4 value, it stands for that the damage state was moderate. In case of S4 and S5 soils (Fig. 8(d) and

500 yrs. of return period	**Case 1** None	**Case 2** None	**Case 3** None	**Case 4** None	**Case 5** Minor	**Case 6** Minor	**Case 7** Minor	**Case 8** Moderate	**Case 9** Moderate	**Case 10** Moderate	**Case 11** Extensive
1000 yrs. of return period	**Case 12** None	**Case 13** None	**Case 14** None	**Case 15** Minor	**Case 16** Minor	**Case 17** Minor	**Case 18** Moderate	**Case 19** Moderate	**Case 20** Moderate	**Case 21** Moderate	**Case 22** Extensive
2400 yrs. of return period	**Case 23** None	**Case 24** None	**Case 25** Minor	**Case 26** Minor	**Case 27** Moderate	**Case 28** Moderate	**Case 29** Moderate	**Case 30** Moderate	**Case 31** Moderate	**Case 32** Extensive	**Case 33** Extensive

Fig. 11 Risk assessment framework based on damage index results

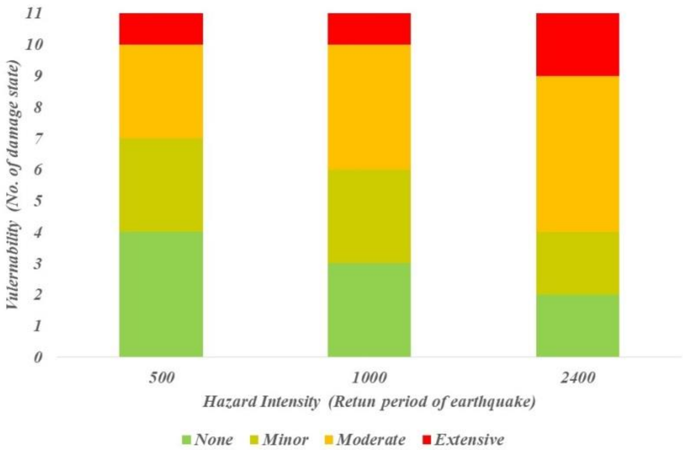

Fig. 12 Damage state of structure according to hazard intensity

8(e)), damage index of all cases was greater than 1.0 value. At least, minor damage could be occurred to the underground structure constructed in S4 or S5 soil deposit. Especially, the damage index of moment in Case 11 exceeded 2.3 value, it implies that the extensive damage could occur as the earthquake with return period of 2,400 years occurred. In this case, the location where maximum bending moment occurs was at the top left corner of the underground railway station.

Effect of soil class and depth of the railway station was explicitly analyzed in Figs. 9 and 10. To investigate effect of soil class, Cases 12, 13, 15, 17, and 20 were plotted in Fig. 9. For cases 13 and 15, soil class was varied (S2 & S3), while other variables were fixed. For cases 17 and 20, soil class was varied (S4 & S5), whereas other variables were fixed and summarized in Table 2. Case 12 was drawn together to show gradual effect of soil class. In Fig. 9, it is identified that damage index increases as soil class varies from S1 to S5. It signifies that when ground has deep and stiff characteristics underground structure is more likely to suffer damage than ground has shallow and stiff characteristics. On the other hand, increment of damage index between S1 and S2, S3, and S4 is less significant than that between S2 and S3, S4, and S5. It can be demonstrated that stiffness of the ground is relatively more dominant for damage index of the underground structure than depth of the base rock. To investigate effect of depth of the railway station, Cases 17, 18, and 19 were plotted in Fig. 10. In these cases, depth of the railway station was only varied (11, 25, and 21m), whereas other variables were fixed. In Fig. 10, it can be identified that damage index increases as depth of the railway structure increases due to the input earthquake characteristics and soil-rock interface effect. It is similar trend with discussion above.

In order to evaluate seismic risk of underground railway station, risk assessment frame work was constructed based on damage index analysis results of bending moment. The column is the return period of earthquake denoting the hazard intensity. The row is the case number standing for site classification and depth of structure. As shown in Fig. 11, the risk index is more severe with increasing the hazard intensity. The risk index is also riskier when site class number and depth of underground structure increased. The structure in S1 and S2 class ground is mostly safe regardless of hazard intensity. In case of S3 class ground, the deep structure could suffer moderate damage by bigger hazard intensity. The deep structures in S4 class ground have possibility suffering moderate damage regardless of hazard intensity. The structures in S5 class ground could be damaged more than moderate state regardless of depth and hazard intensity.

Fig. 12 shows each damage state according to hazard intensity level. In case of return period of 500 years earthquake, 7 of 11 cases are safe and minor damage state. In addition, only one case could suffer extensive damage state by earthquake. However, in case of return period of 2400 years earthquake, 7 of 11 cases are moderate and extensive damage state, and only two cases are safe. It implies that underground structures constructed high earthquake risk area have potential risk due to earthquake. In addition, the structures which required high seismic capacity due to seismic design criteria should consider earthquake risk.

5. Conclusions

Earthquake risk assessment of the railway station structure virtually modeled based on OOO Station in Seoul was carried out by deriving fragility curve based on numerically obtained seismic response of the target system. Followings are detailed concluding remarks.

• Seismic responses of underground railway station were calculated by PLAXIS 2D which is two-dimensional numerical simulation tool for the 33 analysis cases with depth of the base rock, depth of the railway station, and class of input earthquake motion.

• HSSMALL was adopted for soil constitutive model, and interface elements was adopted at the interface between plate and soil element to simulate dynamic interaction effect. Input earthquake motion was artificially created based on recorded values from Pohang earthquake.

• Maximum shear force and bending moment profiles were derived from numerical simulation for every case, and each data was utilized to obtain damage index. The damage index value of deep structure was higher than that of shallow structure. This phenomenon occurred due to input earthquake characteristics and soil-rock interface effect. In addition, cases with lower Vs value shows higher damage index than cases with higher Vs value.

• Based on analysis results, it was concluded that the minor and slight damage could occur on the underground structure constructed in S1, S2 and S3 soil deposit with return period of 1,000 years or 2,400 years earthquakes. However, moderate or extensive damage could occur the structures constructed in S4 and S5 soil deposit even with return period of 500 years earthquake.

• The risk assessment framework was constructed based on damage index analysis results. The risk index is more severe when the hazard intensity increases. The risk index is also riskier when site class number and depth of underground structure increases.

Acknowledgments

This research was supported by a grant from the Review of Environmental Impact Assessment funded by Korea Environment Institute, the R&D Program (PK2002A4) of the Korea Railroad Research Institute, Republic of Korea, and the Basic Science Research Program through the National Research Foundation of Korea(NRF) funded by the Ministry of Education (No. 2018R1A4A1025953) and this was supported by Korea National University of Transportation in 2020.

References

ALA (2001), *Seismic Fragility Formulations for Water Systems Part 1 – Guideline*, American Society of Civil Engineers – FEMA, Chicago, U.S.A.

Andreotti, G. and Carlo, G. (2014), "Seismic vulnerability of deep tunnels: Numerical modeling for a fully nonlinear dynamic analysis", *Proceedings of the 2nd European Conference on Earthquake Engineering and Seismology*, Instanbul, Turkey, August.

Andreotti, G., Lai, C.G. and Martinelli, M. (2013), "Seismic fragility functions of deep tunnels: a new cumulative damage model based on lumped plasticity and rotation capacity", *Proceedings of the International Conference on Earthquake Geotechnical Engineering*, Istanbul, Turkey, June.

Argyroudis, S.A. and Pitilakis, K.D. (2012), "Seismic fragility curves of shallow tunnels in alluvial deposits", *Soil Dyn. Earthq. Eng.*, **35**, 1-12. https://doi.org/10.1016/j.soildyn.2011.11.004.

Corigliano, M., Lai, C.G. and Barla, G. (2007), "Seismic vulnerability of rock tunnels using fragility curves", *Proceedings of the 11th International Society for Rock Mechanics Congress*, Lisbon, Portugal, July.

Dowding, C.H. and Rozan, A. (1978), "Damage to rock tunnels from earthquake shaking", *J. Geotech. Eng. Div.*, **104**(2), 175-191.

Fattah, M.Y., Hamoo, M.J. and Dawood, S.H. (2015), "Dynamic response of a lined tunnel with transmitting boundaries", *Earthq. Struct.*, **8**(1), 275-304. http://doi.org/10.12989/eas.2015.8.1.275.

FEMA, H. (2003), *Multi-Hazard Loss Estimation Methodology, Earthquake Model*, Washington, D.C., U.S.A.

Hashash, Y.M., Hook, J.J., Schmidt, B., John, I. and Yao, C. (2001), "Seismic design and analysis of underground structures", *Tunn. Undergr. Sp. Technol.*, **16**(4), 247-293. https://doi.org/10.1016/S0886-7798(01)00051-7.

Lee, T.H., Park, D., Nguyen, D.D. and Park, J.S. (2016), "Damage analysis of cut-and-cover tunnel structures under seismic loading", *Bull. Earthq. Eng.*, **14**(2), 413-431. https://doi.org/10.1007/s10518-015-9835-x.

Liu, N., Huang, Q.B., Fan, W., Ma, Y.J. and Peng, J.B. (2018), "Seismic responses of a metro tunnel in a ground fissure site", *Geomech. Eng.*, **15**(2), 775-781. https://doi.org/10.12989/gae.2018.15.2.775.

Liu, X.R., Li, D.L., Wang, J.B. and Wang, Z. (2015), "Surrounding rock pressure of shallow-buried bilateral bias tunnels under earthquake", *Geomech. Eng.*, **9**(4), 427-445. https://doi.org/10.12989/gae.2015.9.4.427.

Ministry of Interior and Safety (2017), *Korean Seismic Design Criteria: Common Applications*.

Okamoto, S. (1973), *Introduction to Earthquake Engineering*, University of Tokyo Press, Tokyo, Japan. 29-40.

Ozturk, H.T., Turkeli, E. and Durmus, A. (2016), "Optimum design of RC shallow tunnels in earthquake zones using artificial bee colony and genetic algorithms", *Comput. Concrete*, **17**(4), 435-453. https://doi.org/10.12989/cac.2016.17.4.435.

Park, D., Lee, T.H., Kim, H. and Park, J.S. (2016), "Identification of damage states and damge indices of single box tunnel from inelastic seismic analysis", *J. Kor, Tunn. Undergr. Sp. Assoc.*, **18**(2), 119-128. https://doi.org/10.9711/KTAJ.2016.18.2.119.

Park, D., Nguyen, D.D., Lee, T.H. and Nguyen, V.Q. (2018), "Seismic fragility evaluation of cut-and-cover tunnel", *J. Kor. Geotech. Soc.*, **34**(11), 71-80. https://doi.org/10.7843/kgs.2018.34.11.71.

Pitilakis, K. and Tsinidis, G. (2014), *Performance and Seismic Design of Underground Structures*, Springer International Publishing, New York, U.S.A.

Plaxis, B. (2016), *Reference manual for PLAXIS 2D*, Delft, The Netherlands.

Roy, N. and Sarkar, R. (2017), "A review of seismic damage of mountain tunnels and probable failure mechanisms", *Geotech. Geol. Eng.*, **35**(1), 1-28. https://doi.org/10.1007/s10706-016-0091-x.

Sevim, B. (2013), "Assessment of 3D earthquake response of the Arhavi Highway Tunnel considering soil-structure interaction", *Comput*. *Concrete*, **11**(1), 51-61. https://doi.org/10.12989/cac.2013.11.1.051.

Werner, S.D., Taylor, C.E., Cho, S., Lavoie, J.P., Huyck, C.K., Eitzel, C., Chung, H. and Eguchi, R.T. (2006), "Redars 2 methodology and software for seismic risk analysis of highway systems", Report No. MCEER-060SP08, University of Buffalo, The State University of New York, U.S.A.

CC